Differential measurements of ionization and inelastic energy losses in 0.25–3.0-MeV collisions of Kr ions with Kr and Xe targets

Ali A. Antar* and Quentin C. Kessel
Department of Physics and the Institute of Materials Science, The University of Connecticut, Storrs, Connecticut 06268
(Received 29 July 1983)

The final charge states of the scattered ions and the inelastic energy losses have been measured for single collisions of 0.25–3.0-MeV Kr ions with Kr and Xe targets. The charge states of the scattered ions were measured as functions of scattering angle (from 0.8° to 45°) ion energies from 0.25 to 3.0 MeV. The total inelastic energy losses were measured using the scattered- and recoil-particle coincidence technique for 0.4-, 0.6-, and 1.0-MeV Kr^+-Kr collision energies and from 0.4 to 1.4 MeV for the Kr^+-Xe combination. The results show the impact-parameter dependence of several inner-shell excitations and confirm the quasimolecular nature of heavy-ion–atom collisions within the framework of the Fano-Lichten model. For the Kr-Kr case, excitations are observed for values of the distance of closest approach, R_0, of 0.40, 0.30, and 0.20 Å; and for the Kr-Xe case, excitations are observed at R_0 values of 0.28, 0.18, and 0.09 Å. The data show agreement with the molecular-potential calculations of Eichler and co-workers.

I. INTRODUCTION

The present measurements represent the continuation of a program to extend our knowledge of single-collision phenomena to heavier collision systems at higher energies. During such a collision the electron shells surrounding the two nuclei are forced to interpenetrate, forming a quasimolecule for the duration of the collision. In this collision process, vacancies are often produced in inner shells, sometimes even with a probability of 100% for certain collision conditions. Earlier studies of the lighter Ar^+-Ar system at lower energies[1–3] led to the formulation of a quasimolecular model by Fano and Lichten[4–6] as a framework within which to explain these inner-shell excitations. Several reviews describing these earlier data and the application and remarkable success of Fano and Litchten's molecular-orbital (MO) model have been written.[7–10] In brief, if the relative velocities of the nuclei are less than the characteristic velocities of the electrons in the electron shells under consideration, then the Born-Oppenheimer approximation may be applied to the short-lived quasimolecule formed by the collision. It is then appropriate to speak of radial and rotational coupling of the electronic energy levels of this molecule and the excitations that may be produced by them. As formulated by Fano and Lichten, the model is a one-electron model and the energy levels used to describe the collision are those of a single electron in the field of two modified Coulomb centers. This is expected to be a good approximation for the fast-moving inner-shell electrons which feel the presence of the nuclei most strongly. For the slower-moving outer electrons, better shielded from the nuclei, the model is not expected to hold so well, if at all.

Because the collision velocities are what will determine the range of validity of the model, it is expected that MeV collisions between heavy nuclei, e.g., Xe^+-Xe, Kr^+-Kr, and Kr^+-Xe, will be similar in nature to the keV collisions of the lighter Ne^+-Ne and Ar^+-Ar systems first used to verify the model. The heavy systems already investigated include the quasisymmetric I^{+n}-Xe system[11] and the symmetric Xe^+-Xe system.[12,13] Energy losses of nearly 30 keV were observed to occur in 6-MeV I^{+3}-Xe collisions[14] in which the scattered ion was deflected through 8°. The resulting ionization states were as high as $+27$.[11] Similar ionization states have been observed following smaller-angle scattering of 60-MeV I^{+10} from Xe.[15] These final ionization states reflect the multiple processes which can occur following the production of one or more inner-shell vacancies by the collision. For a deep inner-shell vacancy, cascade effects and Auger-type processes can result in a multiplying factor whereby a single inner-shell vacancy can result in the final charge state increasing by more than one. It is for this reason that the measurement of final charge state of scattered ions as a function of scattering angle becomes a tool for impact-parameter-dependent investigations of inner-shell vacancy production.

Collision energies in the MeV range are required for the investigation of Xe inner-shell excitation by heavy-ion projectiles. Lower collision energies are not sufficient to overcome the Coulomb repulsion of the nuclei and permit the inner electron shells to interact with each other. The detailed study of the Xe^+-Xe system[12,13] investigated only the phenomena of *O*-, *N*-, and *M*-shell ionization; at 1.2 MeV, the *L* shells of the two nuclei did not interpenetrate sufficiently for significant *L*-shell excitation to occur. Coincidence measurements made with Auger electrons and x rays from the Xe^+-Xe system have also been limited to *M*-shell excitations.[16–18] The present investigation of the Kr^+-Kr system does allow interpenetration of the *L* shells. The asymmetric Kr^+-Xe system was included in the study in order to compare the results with MO model generalized by Barat and Lichten for asymmetric collisions.[6] The present data allow for a more detailed com-

parison with the MO model than did earlier data for this combination and confirms the details suggested earlier.[19–21] Other confirmation is found in the recent letter by Shanker and co-workers where x rays are detected in coincidence with the scattered Kr ions[22] and in this laboratory where Auger electrons are being measured in coincidence with the scattered ions.[23]

II. THE EXPERIMENTAL METHOD

The projectile Kr ions are produced in the terminal of a Van de Graaff accelerator, mass analyzed, and directed into a scattering chamber that has been described in a previous paper.[24] The isotope ^{84}Kr (not always fully resolved from the lesser ^{83}Kr component of the beam) passes through differentially pumped 0.76-mm apertures placed 31 cm apart and into the scattering region containing the target gas, either Kr or Xe, with all isotopes present in their natural abundances. A second collimator, using rectangular apertures and subtending an angle of 0.3° from the scattering center in the plane of the apparatus, samples those Kr ions that are scattered through θ degrees by single collisions with the target atoms. Another collimator, also in the scattering plane and subtending an angle of 0.9° from the scattering center, but on the opposite side of the incident ion beam, samples recoil ions emerging from the collision center at an angle ϕ. These latter collimators, together with their associated electrostatic analyzers and particle detectors can each be rotated through a range of angles, θ and ϕ, respectively.

The ionization data are obtained by choosing an ion energy E_0, and scattering angle θ, and electrostatically analyzing the charge of the ions passing through the collimator. After analysis, the number of ions having charge state m, N_m, are counted with a silicon surface-barrier detector. The probability of the ions scattered through the angle θ being found to have charge m is then given by

$$P_m = N_m \Big/ \sum_{m'} N_{m'} \, . \tag{1}$$

At each of several energies the values of P_m were determined for a number of scattering angles for 1–22 deg. For each combination of E_0 and θ and the average charge $\bar{m}$ of the scattered ions was also determined. This is given by

$$\bar{m} = \sum_m m P_m \, . \tag{2}$$

The values of P_m determined this way are single-collision values. The target-gas pressure is kept in the range of $(1-4)\times 10^{-4}$ Torr, and the path length of the ions in the target gas is 2 cm. Tests showed that the final charge states were not seriously affected by multiple collisions until the target-gas pressure was raised above 1×10^{-3} Torr.[25]

To measure the inelastic energy losses for these collisions, delayed-coincidence techniques were used to identify scattered and recoil ions originating from the same collisions. For a given E_0 and θ, the recoil-particle collimator is rotated through a range of angles ϕ. Pulses from the scattered-particle detector are delayed to compensate

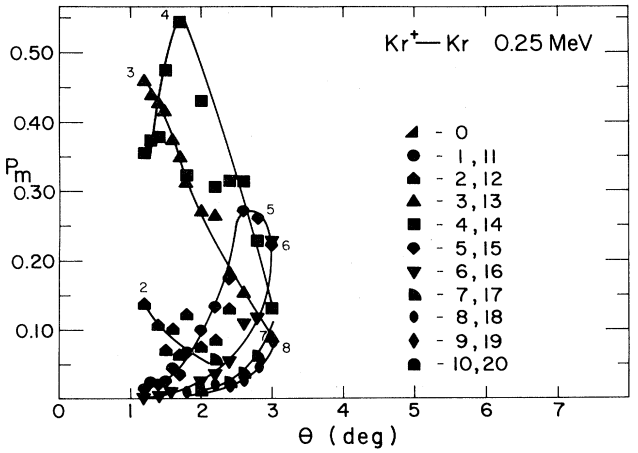

FIG. 1. Probabilities P_m for finding 0.25-MeV ions scattered through θ degrees with charge state m, plotted vs θ. Data scatter is of the same order of magnitude as the size of the symbols themselves. Key for the symbols used for the different m values in Figs. 1–7 and 12–15 is given in the figure. For additional clarity the numbers alongside the curves also indicate the ionization states.

for the different ion time of flight. These pulses, together with those from the recoil-particle detector (an electron multiplier sensitive to the lower-energy recoil ions) are passed through a coincidence circuit. When the angle θ is found for which the maximum number of coincident pulses is observed, this value of ϕ may be used to calculate the average inelastic energy loss $Q = E_0 - E_1 - E_2$ or in terms of E_0, θ, and ϕ,[8]

$$Q = E_0[1 - \sin^2\phi/\sin^2(\theta+\phi) - \gamma \sin^2\theta/\sin^2(\theta+\phi)] \, . \tag{3}$$

Here E_1 and E_2 are the scattered- and recoil-ion energies and γ is the ratio of the incident-ion mass to that of the target-atom mass. Compared to instrumental effects, any variations in Q through γ, due to the different isotopes in the target, may be neglected. Details of this delayed-coincidence technique may be found in Refs. 1 and 3.

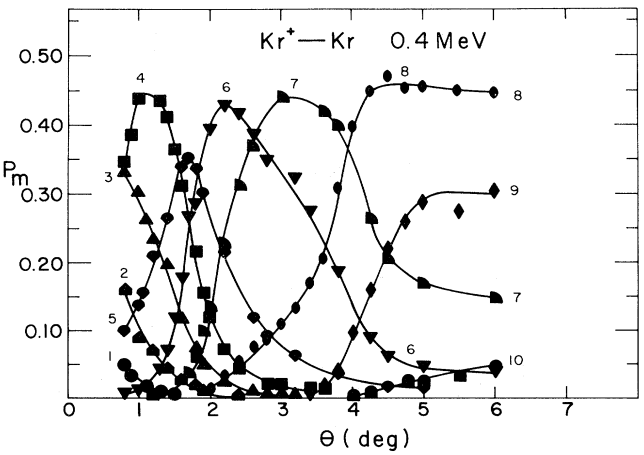

FIG. 2. Similar to Fig. 1 except for the 0.4-MeV data.

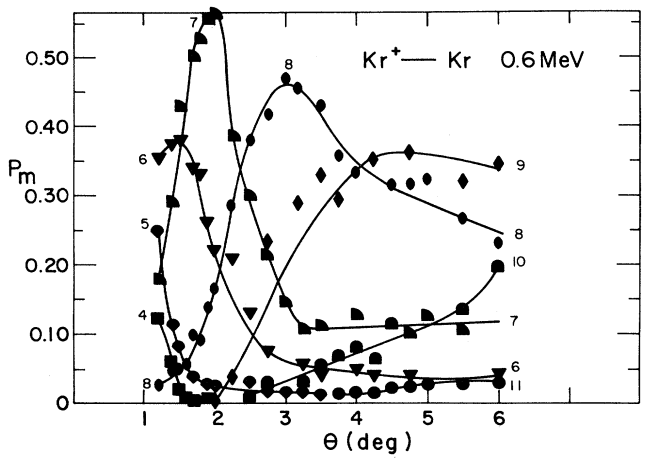

FIG. 3. Similar to Fig. 1 except for the 0.6-MeV data.

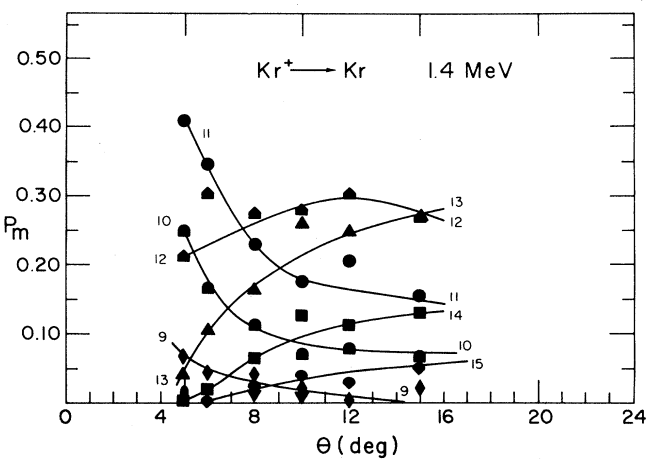

FIG. 5. Similar to Fig. 1 except for the 1.4-MeV data.

III. EXPERIMENTAL RESULTS

Kr^+-Kr ionization data. Figures 1—7 present the probabilities P_m of the scattered ion having charge state m as a function of the scattering angle for collision energies of 0.25, 0.4, 0.6, 1.0, 1.4, 2.0, and 3.0 MeV. The 2.0- and 3.0-MeV data were obtained using doubly ionized Kr ions from the accelerator. The key to the symbols for these figures is given in Fig. 1; additionally, the ionization states are indicated on the figures for each curve. Qualitatively, these curves show the same behavior as similar curves at both lower[26] and higher[11] collision energies for other ion-atom combinations: As either the collision energy or the scattering angle is increased, the degree of ionization increases. These data do not show the obvious irregularities observed in either lower-energy Kr^+-Kr collisions[27] or the 0.25—0.4-MeV Xe^+-Xe collisions.[12] For these latter data it was observed for certain energies and ranges of θ that the P_m values would remain constant or even show irregularities as the average ionization sometimes decreased as θ was increased. An anomaly is observed in the present data for the charge states 5, 6, and 7. The 0.4-MeV data in Fig. 2 show that most of the P_m values reach maximum values of about 45%. The exception is the charge state 5 which peaks at a much lower value. In Fig. 3 the P_6 is low but P_7 reaches nearly 60%. This behavior is probably not due directly to shell structure, but rather to an excitation of the M shell occurring when the product $E_0\theta$ exceeds 0.6. For the less-violent collisions the ionization increases in a continuous fashion, but the excitation at $E_0\theta=0.6$ MeV deg causes a jump in ionization, resulting in P_5 never reaching a maximum greater than 0.35. This excitation will be discussed in greater detail later. Figure 8 plots the $\bar{m}$ values from Figs. 1—7 vs θ. This condensation of the data shows how the average ionization increases as either E_0 or θ is increased.

In Fig. 9 these same $\bar{m}$ data are plotted, but this time versus the product $E_0\theta$. This product is useful because for the angles under consideration here there is nearly a one-to-one relationship between the $E_0\theta$ value of a given collision and that collision's value of R_0, the distance of closest approach of the two nuclei.[28] Approximate values of R_0 are also given in Fig. 9. At $E_0\theta=0.2$, 0.6, 1.0, and 1.7 MeV deg, $\bar{m}$ is observed to increase nonmonotonically.

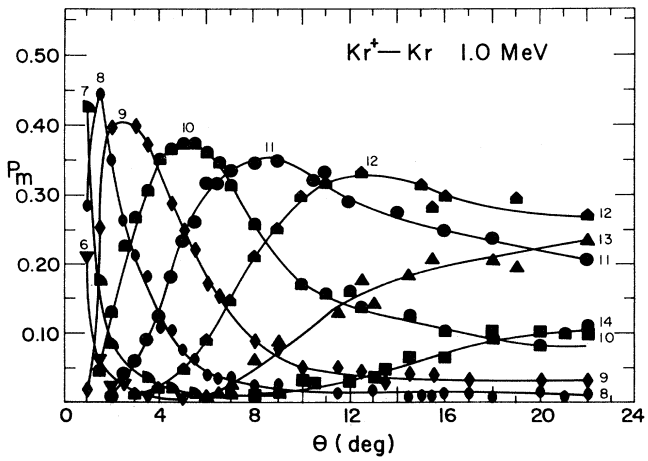

FIG. 4. Similar to Fig. 1 except for the 1.0-MeV data.

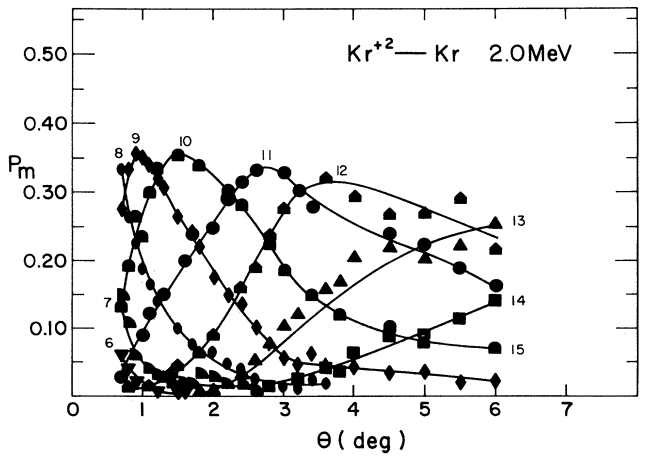

FIG. 6. Similar to Fig. 1 except for the 2.0-MeV data. Kr^{+2} ions from a 1-MV potential were used to obtain 2-MeV incident ion energy.

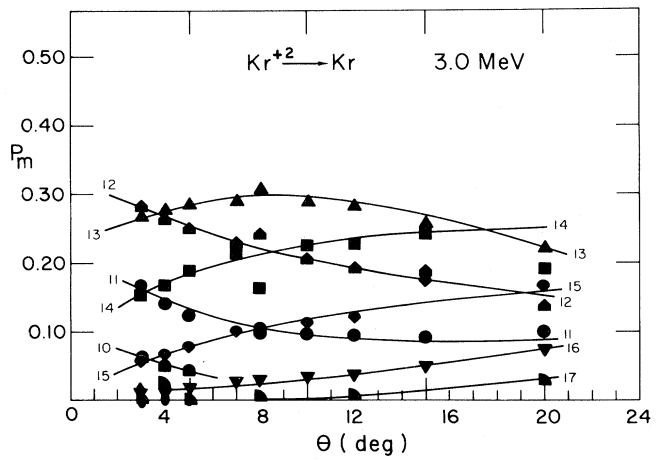

FIG. 7. Similar to Fig. 6 except for the 3.0-MeV data.

For larger values of $E_0\theta$, $\bar{m}$ continues to increase with only a suggestion of possible irregularities. Afrosimov and co-workers observed similar increases at 0.2, 0.6, and 1.0 MeV deg for 50-keV scattering.[27] McCaughey and co-workers[29,30] and Fastrup and Herman[31] have studied the excitation at 0.2 MeV deg in detail and it may be attributed the promotion of two $3d$ electrons via the diabatic $6h\sigma$ MO.[8]

Kr^+-Kr Q-value data. In Fig. 10 the Q values corresponding to ionization data in Fig. 9 are plotted; also included are the lower-energy data of McCaughey and co-workers.[29] As will be pointed out in the following discussion, it is through a comparison of these two figures that information on the underlying excitations may be derived. For example, in going from $E_0\theta=0.3$ to 1.0 MeV deg $\bar{m}$ increases by 3 and Q by only a few hundred eV. On the other hand, between 5 and 20 MeV deg $\bar{m}$ increases by only 2 while Q increases by 3 keV. This is shown more clearly in Fig. 11 which plots the Q values from Fig. 10 against the $\bar{m}$ values of Fig. 9. These different orders of magnitude in the excitation energy are typical of those expected for promotions of electrons from shells of different

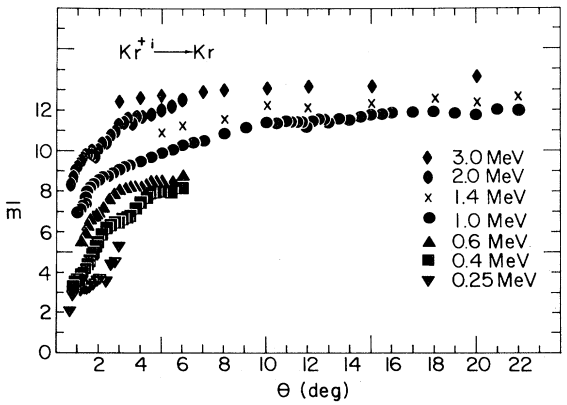

FIG. 8. Average charge state $\bar{m}$ of the scattered ions plotted vs the scattering angle θ for the Kr^+-Kr collisions. Sum of the electrons lost from both the target and the projectile during the collision is estimated to be $2\bar{m}-1$.

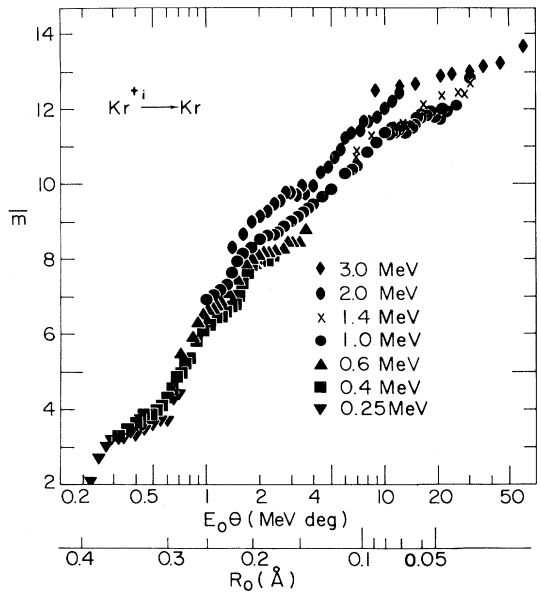

FIG. 9. The average charge state $\bar{m}$ plotted vs the product $E_0\theta$ for the data in Fig. 8. Separate curves are shown for each of the energies, and approximate values of R_0 are also shown along the abscissa.

principal quantum number.

Kr^+-Xe ionization data. Figures 12—15 present the P_m values for the 0.4-, 0.6-, 1.0-, and 3.0-MeV Kr^+-Xe collisions. The key for these symbols is also given in Fig. 1, and, for clarity, the ionization states are indicated on the figures for each curve. The data are similar in nature to those for Kr^+-Kr; however, here it is the $+7$ curve which is suppressed in the 0.6-MeV data. Again this anomaly may be associated with a shell excitation occurring at about 2.5 MeV deg. It might be noted that the

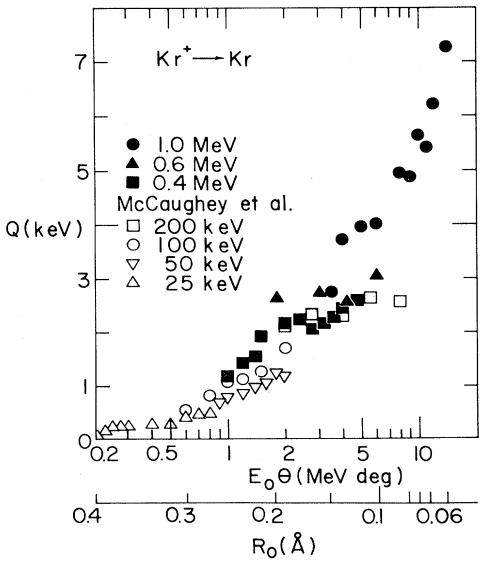

FIG. 10. Inelastic energy loss Q plotted vs $E_0\theta$ with the approximate values of R_0 indicated. Also given are data from Ref. 29.

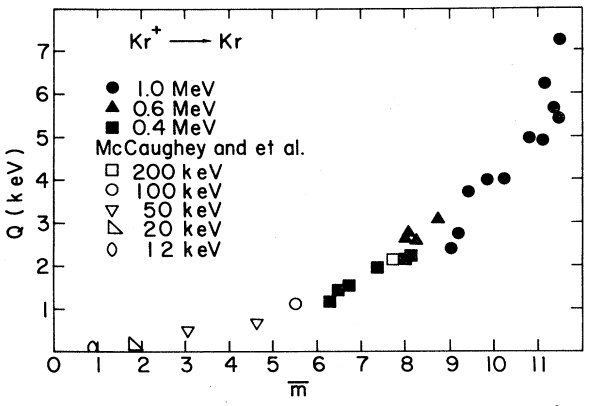

FIG. 11. Data of Figs. 9 and 10 displayed in a plot of Q vs $\bar{m}$. Included are data from Ref. 29.

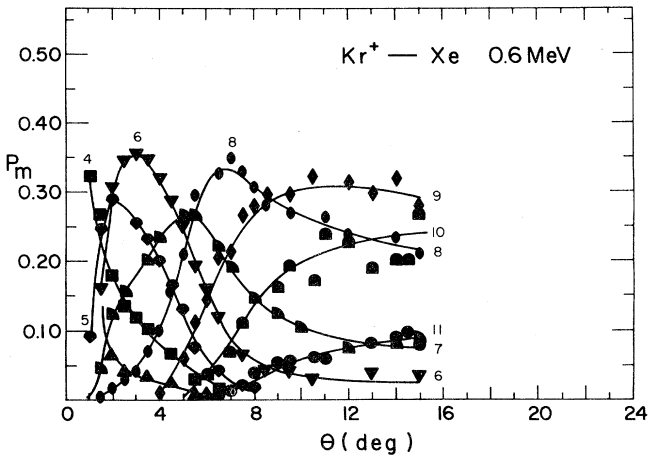

FIG. 13. Similar to Fig. 1 except for the 0.6-MeV Kr^+-Xe collisions.

suppression occurs for the $+7$ in Kr^+-Xe collisions and for the $+5$ or $+6$ in the Kr^+-Kr collisions. This indicates that the anomaly is not associated with levels in the Kr atom itself, but with the collision system as a whole. Figure 16 plots $\bar{m}$ vs θ. Again, $\bar{m}$ increases with either increasing collision energy or scattering angle; however, the irregularities in the curve show no systematic behavior until they are plotted versus $E_0\theta$ or R_0. This is done in Fig. 17, and shows clear evidence for three excitations. These excitations have onsets at 0.7, 2.0, and 10.0 MeV deg, corresponding to approximate R_0 values of 0.3, 0.2, and 0.1 Å, respectively.

Kr^+-Xe Q-value data. The Q values for a subset of the data of Fig. 17 are shown in Fig. 18. Experimental limitations precluded obtaining data for lower values of E_0 and θ. The steps in these data have thresholds at 3.0 and 10 MeV deg and correspond to the upper two excitations of Fig. 17. Comparing these two figures, it is observed that the excitation at 0.7 MeV deg corresponds to an increase in charge state of 2.5 for the scattered Kr ion, but of a loss that must be less than 1 keV. The other two each result in an increase in $\bar{m}$ of about 3. The increase in Q for the $E_0\theta=2.0$ MeV deg excitation is 3 keV and for the 10-MeV deg excitation, about the same or larger. The Q values appear to level off, or even decline above 25 MeV deg and there is a corresponding leveling off of the $\bar{m}$ values in Fig. 17. The error bars in Fig. 18 correspond to an uncertainty of 0.02 deg in the measurement and calculation of Q [Eq. (3)]. Whereas for low values of E_0 and θ this contributes little to the uncertainty of the measurements, beyond $E_0\theta=25$ MeV deg it becomes a significant factor.

IV. DISCUSSION

This discussion will be carried out within the framework provided by Fano and Lichten[4] with their one-electron model. The MO's used by Lichten and coworkers[5,6] are termed diabatic MO's and are based on the behavior expected of a single electron in the field of two screened Coulomb potentials. This avoids direct consideration of the electron-electron interactions responsible for the avoided or pseudocrossings of MO's of like symmetry found in all adiabatic calculations of multielectron

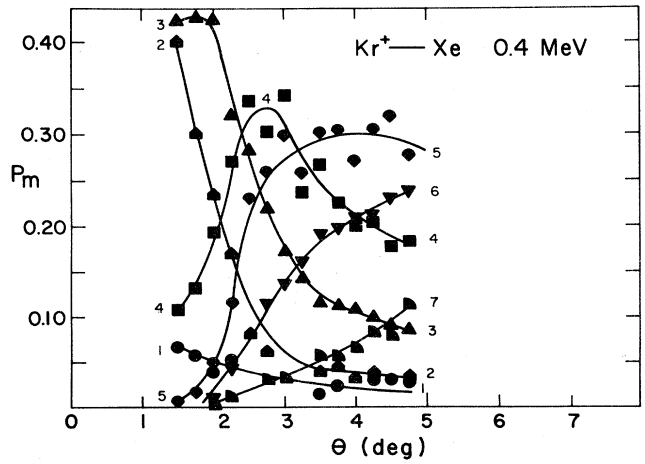

FIG. 12. Similar to Fig. 1 except for the 0.4-MeV Kr^+-Xe collisions.

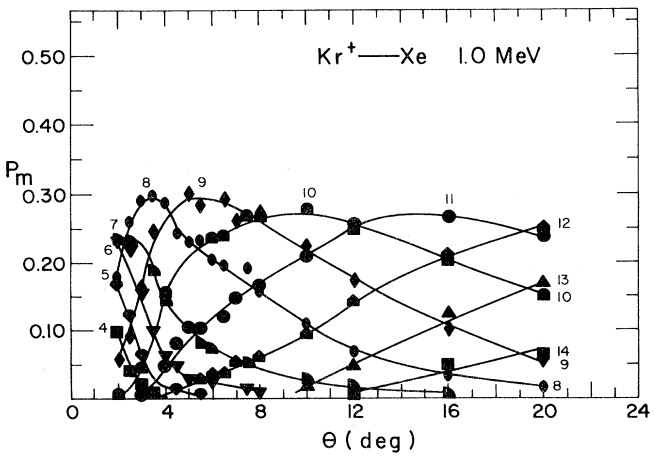

FIG. 14. Similar to Fig. 1 except for the 1.0-MeV Kr^+-Xe collisions.

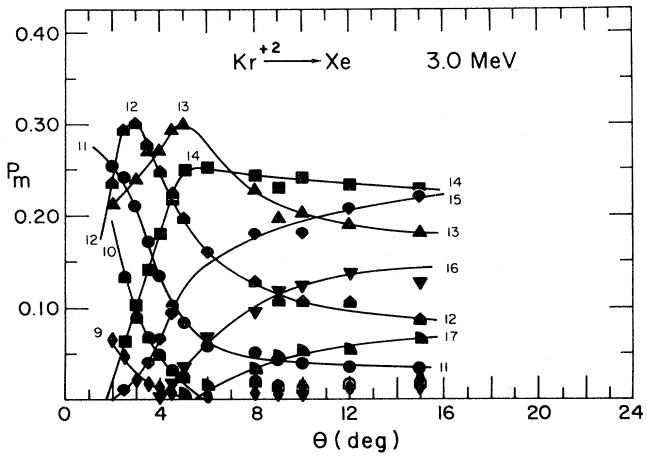

FIG. 15. Similar to Fig. 7 except for the 3.0-MeV Kr^{+2}-Xe collisions.

systems. The diabatic orbitals may, however, be considered dynamic orbitals resulting from the perturbation of the adiabatic orbitals. For this reason, it is appropriate to base the following discussion on the adiabatic calculations of Eichler and co-workers,[32] and the results of these calculations for the Kr-Kr and Kr-Xe molecules are shown in Figs. 19 and 20. This does lead to a certain confusion in the nomenclature used for identifying individual potential curves. In the adiabatic case it is convenient to identify them as σ, π, or δ, gerade or ungerade states by simply counting up from the lowest level i.e., $1\sigma_g$, $1\sigma_u$, $2\sigma_g$, $2\sigma_u$, etc. Because of the noncrossing rule, this leads to a relatively simple labeling system. On the other hand, this is not practical for diabatic diagrams and Lichten adopted the united-atom designation for the specification of diabatic curves. For example, in this notation the Kr-Kr $4f\sigma$ level would connect the united-atom (UA) $4f$ level with the separated-atom (SA) $2p$ level. The diabatic $4f\sigma$ level is thus the continuous potential curve made by joining sections of the adiabatic $3\sigma_u$ and $4\sigma_u$ curves. Thus a collision can "promote" an electron from the SA $n=2$ level to a UA $n=4$ level via the diabatic $4f\sigma$ level in this

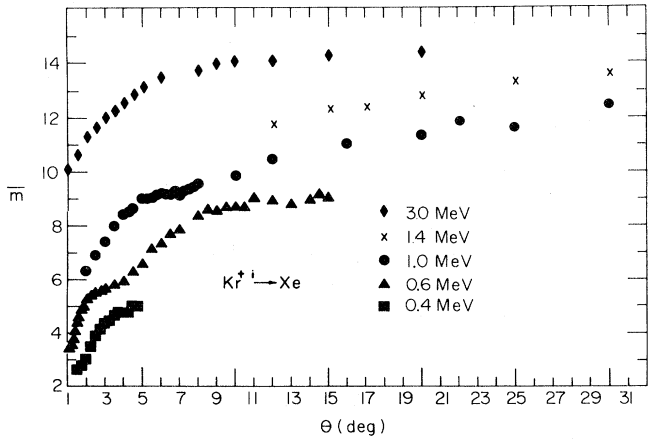

FIG. 16. Average charge state $\bar{m}$ for the scattered Kr ion plotted vs θ for the Kr^{+}-Xe collisions.

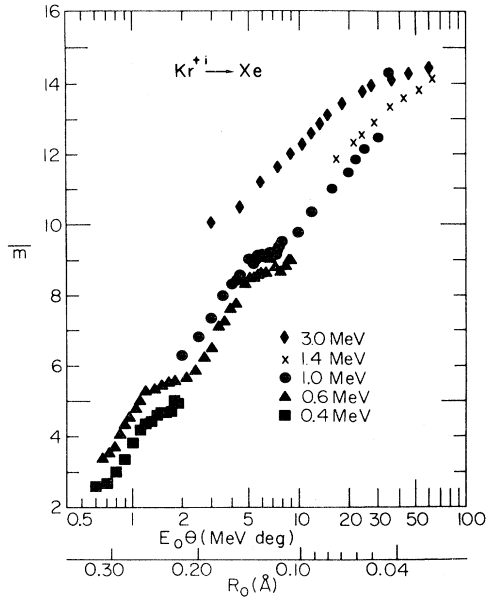

FIG. 17. Average charge state $\bar{m}$ of the scattered Kr ion plotted vs $E_0\theta$ for Kr^{+}-Xe collisions. Separate curves are shown for each of the energies, and approximate values of R_0 are also shown along the abscissa.

example. This is a physically appropriate connection because radial coupling, due to the motion of the nuclei, make it highly probable that an electron's energy will be most accurately described by the $4f\sigma$ curve during a collision. Where necessary for clarity, both designations will be given in this paper.

The Kr^{+}-Kr collision. The first of the excitations evident in the $\bar{m}$ data of Fig. 9 is the rise occurring at $E_0\theta=0.2$ MeV deg, corresponding to an $R_0=0.40$ Å. It should be noted that $\bar{m}-1$ gives the average number of electrons lost by the scattered ion. It has been shown for other symmetric collision systems that the average charge

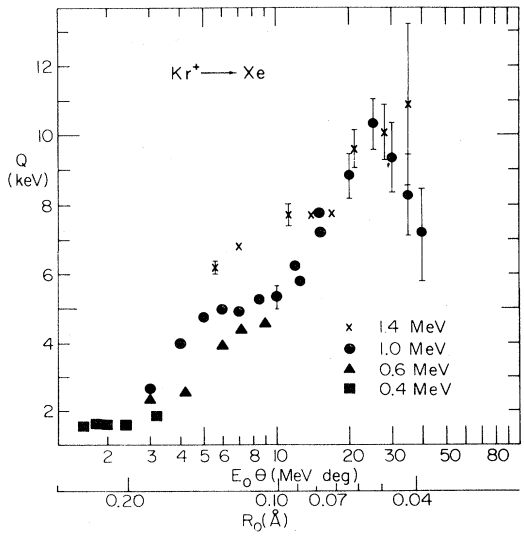

FIG. 18. Inelastic energy loss Q plotted vs $E_0\theta$ with the approximate values of R_0 indicated.

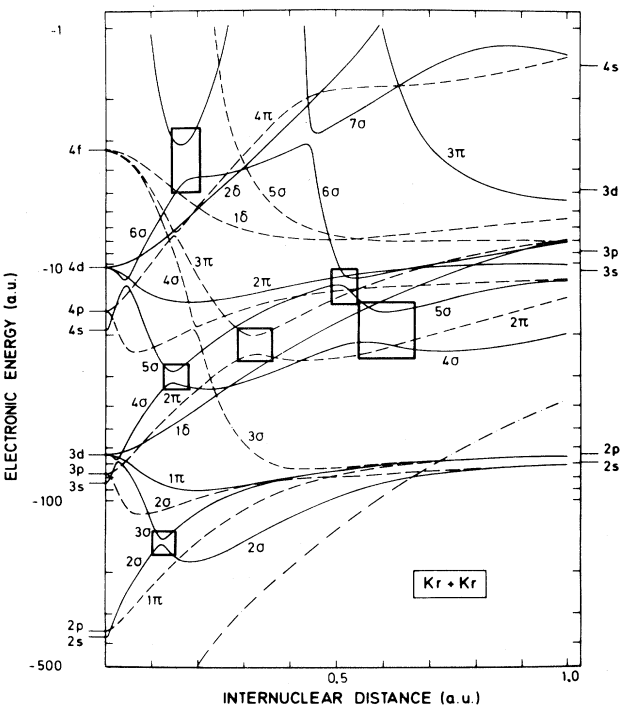

FIG. 19. Adiabatic molecular-potential calculations by Eichler and co-workers for the Kr-Kr system (Ref. 32). Electronic energies are given in a.u. along the ordinate. Along the abscissa the internuclear distance is also given in a.u. Since a length of two a.u. is equal to one Å, the values along the abscissa should be divided by two before comparing with the R_0 values given in this paper. Boxes indicate possible couplings not included in the "Barat-Lichten rule."

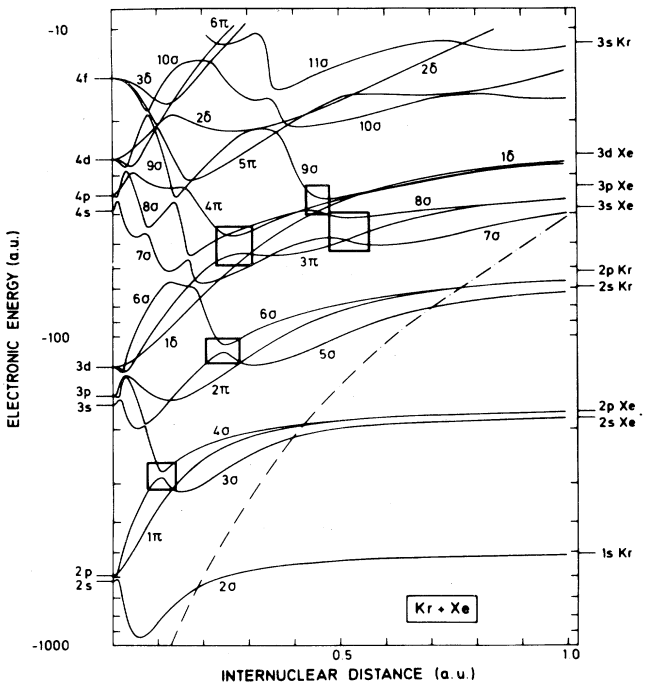

FIG. 20. Calculations by Eichler and co-workers (Ref. 32) for the Kr-Xe system. See the caption to Fig. 19 for further explanation.

of the recoil ion usually equals that of the scattered ion, i.e., the total number of electrons lost is $2\bar{m}-1$.[3,7] This excitation was identified by Fastrup and Herman[31] as being due to the promotion of two $3d$ electrons from the M shells of the Kr atoms. The binding energy of this level is 90 eV,[33] a figure consistent with the energy-loss value of about 200 eV for these data. The first MO capable of promoting $3d$ electrons is the adiabatic $6\sigma_u$ (the diabatic $6h\sigma$) level which is not shown in Fig. 19. However, Ref. 18 does include this level in the Xe-Xe diagram presented there, and it experiences a sharp promotion at 0.25 Å. Simple $1/Z$ scaling gives an estimate of 0.38 Å as the R_0 value at which it would experience a similar promotion for the Kr-Kr case. Therefore, all data indicate this excitation as being the promotion of two $3d$ electrons along the diabatic $6h\sigma$ MO.

The second excitation in Fig. 9 occurs between $E_0\theta=0.6$ and 1.0 MeV deg, corresponding to R_0 values from 0.30 to 0.25 Å. The Q values in this region continue to increase gradually, but Fig. 11 shows that the energy lost per ionization is similar to that for the promotion of the two $3d$ electrons already discussed. Therefore, it is reasonable to look for another MO originating in the SA $3d$ level to explain the ionizations. Reference to Fig. 19 shows that the $3\pi_g$ MO (the diabatic $5g\pi$ MO) fits the description: it originates in the SA $3d$ level and is sharply promoted between 0.3 and 0.25 Å (1 a.u.=0.5 Å).

The third excitation in Fig. 9 occurs at $E_0\theta=1.7$ MeV deg, corresponding to $R_0=0.20$ Å. Here $\bar{m}$ is about 8 and the slope in Fig. 11 is about double what it was for the electrons promoted from the $3d$ shell. While this excitation must still originate in the M shell (the $2p$ binding energy is about 1700 eV as opposed to 90 eV for the $3d$ shell and about 220 eV for the $3p$ shell) neither the data nor Fig. 19 provide definite information as to which subshell the vacancy is produced in. A diabatic MO rising dramatically at 0.20 Å (0.4 a.u.) can be constructed from the gerade 6σ and 7σ MO's in Fig. 19. However, the SA limit of the diabatic MO so constructed is not clear. Possible couplings, indicated by the boxes in the figure, would allow the promoted electrons to originate in either the $3s$, $3p$, or $3d$ level. This laboratory is presently undertaking coincidence measurements between the resulting Auger electrons and the scattered ions in order to provide further information on this.

Figures 10 and 11 suggest the presence of a fourth excitation. The slope in Fig. 11 increases dramatically at $\bar{m}=11$ with Q increasing by as much as 2 keV for an increase in $\bar{m}$ of less than one. Reference to Fig. 9 shows that $\bar{m}=11-12$ corresponds to a range in $E_0\theta$ of 10–20 MeV deg and in R_0 of from 0.08 to 0.05 Å. Both this range of R_0 and the order of magnitude of the Q values suggest that this excitation corresponds to the promotion of $2p$ electrons along the $3\sigma_u$-$4\sigma_u$ path (the diabatic $4f\sigma$ MO), consistent with the results of Ref. 22.

The Kr^+-Xe collision. The first of the excitations observed in Fig. 17 is centered about $E_0\theta=0.9$ MeV deg or $R_0\cong 0.28$ Å. The $\bar{m}$ for the scattered ion increases from 2.5 to 5. Reference to Fig. 20 shows that the only likely

possibilities for promoting Kr electrons are from the $n=2$ and 3 shells. The $n=2$ shell may be eliminated from consideration because the Q values for these collisions are 1 keV or less and the $2p$ binding energy of Kr is about 1700 eV. This leaves the $n=3$ shell which is only partially shown in Fig. 20. The most likely explanation for this excitation is the promotion of Kr $3d$ electrons by the diabatic $6h\sigma$ MO whose promotion may be expected to occur in this range of R_0.[25]

The second excitation, centered at $E_0\theta=3.0$ MeV deg or $R_0\cong 0.18$ Å, results in an increase in $\bar{m}$ of 3.5 and in Q of about 2 keV. The Q value could be accounted for by the promotion of one or two electrons from the $n=3$ shell of Xe which has binding energies of about 1000 eV; it is unlikely that the $n=3$ shell of Kr, with binding energies of 90–220 eV could account for this loss. Sections of the adiabatic 7σ, 8σ, 9σ, 10σ, and 11σ MO's can be pieced together to form a highly promoted diabatic $5g\sigma$ MO at the correct value of R_0. However, the data in Fig. 17 pertain to the scattered Kr ions and would not reflect such an excitation of the Xe target. The present data provide no definitive explanation of this excitation. It would appear that Xe $n=3$ electrons have to be promoted in order to account for the increased energy loss. At the same time, perhaps, some of the collisions may result in promotion of $n=3$ Kr electrons. These might, in a certain fraction of the collisions be promoted along the $5g\sigma$ MO or along some MO not shown in Fig. 20. Coincidence measurements are being undertaken by this laboratory in an attempt to provide further information on this matter.[23]

The third excitation, centered at $E_0\theta=13$ MeV deg or $R_0=0.09$ Å is also accompanied by an increase in Q of 2 or 3 keV. In this case there is an appropriate diabatic MO, the $4f\sigma$, comprised of sections of the adiabatic 5σ, 6σ, 7σ, 8σ, and 9σ, and 10σ MO's.[22] This is highly promoted near $R_0=0.09$ Å and the binding energy of the $n=2$ shell of Kr 1600–1900 eV. The original prediction of Barat and Lichten is that such an $n=2$ electron would originate from the Kr $2p$ shell. On the other hand, the coupling between the 5σ and 6σ levels (indicated by a box in Fig. 20) caused Eichler and co-workers to predict that the promoted electron will be from the $2s$ shell. Electron spectra showing the presence of electrons with energies in the 190–600-eV range for both Kr^+-Kr and Kr^+-Xe are consistent with this latter prediction.[34,35] Coster-Kronig electrons resulting from the filling of a $2s$ vacancy from the $2p$ level of the Kr during the collision could have energies in this range. Another suggestion, by Woerlee and co-workers, is that ejected electrons in this range might be the result of direct coupling with the continuum.[36]

V. SUMMARY

The experiment has provided information on a number of inner-shell excitations through the observation of the ionization states of the scattered projectiles and the related inelastic energy losses. The shells probed were the M and L shells for the Kr^+-Kr collisions and the Kr M and L shells and the Xe M shell for the Kr^+-Xe collisions. With the aid of calculations from Eichler and co-workers it is sometimes possible to extract information on the specific subshell from which the electron was promoted. The analysis, within the remarkable framework provided by Fano and Lichten, confirms the validity of their model for the description inner-shell excitations in these very-heavy-ion–atom collision at MeV energies.

ACKNOWLEDGMENT

This research was supported by National Science Foundation Grant No. PHY-81-06915.

*Permanent address: Central Connecticut State University, New Britain, CT 06050.

[1]V. V. Afrosimov, Yu. S. Gordeev, M. N. Panov, and N. V. Fedorenko, Zh. Tekh. Fiz. 34, 1613 (1964) [Sov. Phys.—Tech. Phys. 9, 1248 (1965)]; 34, 1624 (1964) [9, 1256 (1965)]; 34, 1637 (1964) [9, 1265 (1965)].

[2]Q. C. Kessel, A. Russek, and E. Everhart, Phys. Rev. Lett. 14, 484 (1965).

[3]Q. C. Kessel and E. Everhart, Phys. Rev. 146, 16 (1966).

[4]U. Fano and W. Lichten, Phys. Rev. Lett. 14, 627 (1965).

[5]W. Lichten, Phys. Rev. 164, 131 (1967); J. Phys. Chem. 84, 2102 (1984).

[6]M. Barat and W. Lichten, Phys. Rev. A 6, 211 (1972).

[7]Q. C. Kessel, Case Stud. At. Phys. 1, 399 (1969).

[8]Q. C. Kessel and B. Fastrup, Case Stud. At. Phys. 3, 137 (1973).

[9]J. D. Garcia, R. J. Fortner, and T. M. Kavanagh, Rev. Mod. Phys. 45, 111 (1973).

[10]W. Meyerhof and K. Taulbjerg, Ann. Rev. Nucl. Sci. 27, 279 (1977).

[11]Q. C. Kessel, Phys. Rev. A 2, 1881 (1970).

[12]R. A. Spicuzza and Q. C. Kessel, Phys. Rev. A 14, 630 (1976).

[13]R. A. Spicuzza, A. A. Antar, and Q. C. Kessel, Phys. Rev. A 18, 776 (1978).

[14]Q. C. Kessel, P. H. Rose, and L. Grodzins, Phys. Rev. Lett. 22, 1031 (1969).

[15]L. N. Bridwell, J. A. Biggerstaff, G. D. Alton, C. M. Jones, P. D. Miller, Q. C. Kessel, and B. Wehring, in *Proceedings of the Fourth International Conference on Beam-foil Spectroscopy and Heavy-Ion Atomic Physics, Gatlinburg, Tennessee, 1975* (Plenum, New York, 1976), pp. 657–664.

[16]A. Antar, P. Clapis, J. Gianopoulos, D. Olson, R. Rubino, G. Thomson, and Q. C. Kessel, in *Proceedings of the 12th International Conference on Physics of Electronic and Atomic Collisions, Gatlinburg, Tennessee, 1981,* edited by S. Datz (ICPEAC, Gatlinburg, 1981), pp. 866 and 867.

[17]R. Shanker, R. Hippler, U. Wille, and H. O. Lutz, in Ref. 16, pp. 868 and 869.

[18]R. Shanker, R. Hippler, U. Wille, and H. O. Lutz, J. Phys. B 15, 2041 (1982).

[19]Q. C. Kessel and A. A. Antar, in *Proceedings of the Tenth International Conference on the Physics of Electronic and Atomic Collision* (Commissariat à l'Energie Atomique, Paris, 1977), pp. 18 and 19.

[20]A. A Antar and Q. C. Kessel, Bull. Am. Phys. Soc. 23, 1107 (1978); 24, 580 (1979).

[21]A. A. Antar and Q. C. Kessel, IEEE Trans. Nuc. Sci. NS-28, 1230 (1981).

[22]R. Shanker, R. Hippler, U. Wille, R. Bilau, and H. O. Lutz, J. Phys. B 15, L495 (1982).

[23]P. Clapis, R. Roser, and Q. Kessel, Bull. Am. Phys. Soc. (to be published).

[24]Q. C. Kessel, Rev. Sci. Instrum. 40, 68 (1969). The authors are grateful to High Voltage Engineering Corporation, Burlington, Mass., for making the chamber available for this investigation.

[25]A. A. Antar, Ph.D. thesis, University of Connecticut, 1977.

[26]E. N. Fuls, P. R. Jones, F. P. Ziemba, and E. Everhart, Phys. Rev. 118, 1552 (1960).

[27]V. V. Afrosimov, Yu.S. Gordeev, M. N. Panov, and N. V. Fedorenko, Zh. Tekh. Fiz. 36, 123 (1966) [Sov. Phys.—Tech. Phys. 11, 89 (1966)].

[28]E. Everhart, G. Stone, and R. J. Carbone, Phys. Rev. 99, 1287 (1955). The R_0 values used in this paper are calculated using a screened Coulomb potential. See also F. W. Bingham, J. Chem. Phys. 46, 2003 (1967).

[29]M. P. McCaughey, E. J. Knystautas, H. C. Hayden, and E. Everhart, Phys. Rev. Lett. 21, 65 (1968).

[30]M. P. McCaughey, E. J. Knystautas, and E. Everhart, Phys. Rev. 175, 14 (1968).

[31]B. Fastrup and G. Hermann, Phys. Rev. A 3, 1955 (1971).

[32]J. Eichler, U. Wille, B. Fastrup, and K. Taulbjerg, Phys. Rev. A 14, 707 (1976).

[33]The binding energies given in this article have been obtained from or extrapolated from tables in J. A. Bearden and A. F. Burr, Rev. Mod. Phys. 31, 49 (1967). They can only be used as estimates of the actual binding energies in the present situation.

[34]P. Clapis, A. Antar, S. Kuptsov, R. Roser, R. Rubino, and Q. Kessel, *Book of Abstracts: XII International Conference on the Physics of Electronic and Atomic Collisions, Berlin, 1983,* edited by J. Eichler, W. Fritsch, I. V. Hertel, N. Stoiterfoht, and U. Wille (ICPEAC, Berlin, 1983), p. 475.

[35]Yu. S. Gordeev, P. H. Woerlee, H. de Waard, and F. W. Saris, J. Phys. B 14, 513 (1981).

[36]P. H. Woerlee, Yu. S. Gordeev, H. de Waard, and F. W. Saris, J. Phys. B 14, 527 (1981).